Urban Climate 34 (2020) 100700

Contents lists available at ScienceDirect

Urban Climate

journal homepage: www.elsevier.com/locate/uclim

Investigating the diversity of land surface temperature characteristics in different scale cities based on local climate zones

Jun Yang[a,*], Yixuan Zhan[a,b], Xiangming Xiao[c], Jianhong Cecilia Xia[d], Wei Sun[e,**], Xueming Li[f]

[a] *Human Settlements Research Center, Liaoning Normal University, Dalian 116029, China*
[b] *Jangho Architecture College, Northeastern University, Shenyang 110169, China*
[c] *Department of Microbiology and Plant Biology, Center for Spatial Analysis, University of Oklahoma, Norman, OK 73019, USA*
[d] *School of Earth and Planetary Sciences (EPS), Curtin University, Perth 65630, Australia*
[e] *Nanjing Institute of Geography and Limnology, Key Laboratory of Watershed Geographic Sciences, Chinese Academy of Sciences, Nanjing 210008, China*
[f] *Human Settlements Research Center, Liaoning Normal University, 116029 Dalian, China*

A R T I C L E I N F O

Keywords:
Local climate
City size
Urban heat island effect
Land surface temperature
Pearl river delta urban agglomeration

A B S T R A C T

The concept of Local Climate Zones (LCZs) are effective tools to quantify the urban heat island effect. However, the study of LCZs mainly focuses on the meso-micro scale, and lacks regional perspective. In order to explore the thermal environment laws of different sized cities, we selected the Pearl River Delta urban agglomerations as the study area, and used multi-source data and spatial analysis methods to obtain the thermal environment characteristics of each city based on LCZs. Our study revealed that the distribution of buildings and the relief slope affects land surface temperature (LST). Additionally, the proportions of various LCZs are different in cities of different sizes; each city had a temperature difference in the LCZs. The highest temperature among the built LCZs was in LCZ 7 (Industry; 21.810 °C), whereas the temperature of LCZ A (Dense trees) was the lowest (15.670 °C), and larger cities had more high-temperature LCZs. In cities of different sizes, the temperature of LCZs showed a hierarchy effect, i.e., super cities > megacities > type I large cities > type II large cities. Therefore, in order to alleviate the urban heat island effect, it is of great significance to discover the thermal environment characteristics in cities of different sizes.

1. Introduction

Abnormal climate changes and extreme weather events have increased the harmful effects of environmental pollution and local climate change and are threatening the habitats of humans and other species (Yang et al. 2015; Zhao et al. 2015; Lutz 2017; Miller et al. 2018; Albert et al. 2019; Hong et al. 2019). Canadian meteorologist T. R. Oke proposed the idea of the urban climate zone (UCZ) at the World Meteorological Congress in 2004, from which Stewart and Oke derived the concept of the Local Climate Zones (LCZs) (Stewart and Oke 2012). The classification of LCZs is similar to the classification of the degree of impact of land surface features on

* Corresponding author at: Human Settlements Research Center, Liaoning Normal University, Dalian 116029, China.
** Correspondence to: Nanjing Institute of Geography and Limnology, Key Laboratory of Watershed Geographic Sciences, Chinese Academy of Sciences, Nanjing 210008, China.
E-mail addresses: yangjun8@mail.neu.edu.cn (J. Yang), xiangming.xiao@ou.edu (X. Xiao), c.xia@curtin.edu.au (J.C. Xia), wsun@niglas.ac.cn (W. Sun).

https://doi.org/10.1016/j.uclim.2020.100700
Received 18 April 2020; Received in revised form 16 September 2020; Accepted 16 September 2020
2212-0955/

the urban heat island effect, which can be used to identify the areas that urgently require heat alleviation.

China has the highest annual carbon dioxide emissions in the world, and its rapid rate of urbanization has significantly altered land use patterns. This has affected the energy consumption of residential units, and the urban heat island effect is prominent in many cities (Cui and Shi 2012; Fang et al. 2018; Kang 2013; Qiao et al. 2019; Yang et al., 2017; Yue et al. 2012). The Chinese government issued the Action Plan for Urban Adaptation to Climate Change in 2016, which incorporates climate change indicators into the urban and rural planning system and involves the construction of pilot cities that are adaptive to climate change (MOHURD 2016). The application of the LCZ concept provides a new perspective and method of studying the urban heat island effect and promotes the combination of climate science research and policy planning (Brousse et al. 2019; Natasha and Alicia 2019; Yang et al., 2019a; Emmanuel et al. 2020). Therefore, we conducted research using LCZs to quantify the temperature differences among various types of land surface features.

LCZs can aid the understanding of the distribution of the thermal environment corresponding to different land surface characteristics and can be used to display urban climate conditions spatially (Chen and Tang 2017; Lin and Xu 2017). In this way, our study using LCZs serves as a tool to quantify the thermal environment of the Pearl River Delta urban agglomeration. Before comparing the thermal environment of cities of different sizes, LCZs mapping is required. Some researchers designed parameters when performing LCZs mapping, and identified and described LCZ types by developing GIS and establishing a database for LCZs identification (Lelovics et al. 2013, 2014; Bechtel et al. 2015). In our study, we used detailed building data to classify the LCZ regarding land use type. We found that this method was consistent with the actual situation. However, when the LCZs are classified in different cities, the classification efficiency tends to be relatively low due to the differences in development status in different cities. Some researchers have also developed the World City Database Portal Tool (WUDAPT) project which used remote sensing data to set uniform standards with which to classify a large number of cities in a short space of time (Cai et al. 2016; Danylo et al. 2016; Kotharkar and Bagade 2017; Shi et al. 2018; Wang et al. 2018). Although the project improved efficiency, it suffered from low accuracy.

At present, LCZs are usually applied at mesoscale and microscale. On the one hand, it is used for model prediction studies and has been combined with various analysis methods to assess the urban thermal environment and predict outdoor temperature changes in urban spaces (Zhan et al. 2012; Yvonne 2015; Chen et al. 2017; Jan et al. 2018; Pacifici et al. 2019). On the other hand, LCZs are also used in climate model simulations to evaluate the response of various types of land features to the urban heat island effect (Quan et al. 2016; Marie-Leen et al. 2018; Perera and Emmanuel 2018; Franco et al. 2019). In contrast, our study selected a regional scale research area and used LCZs to quantify the LST results in order to compare the thermal environment of cities of different sizes. Each city has its own unique surface structure and land use status. At different times of the day, surface cover plays a different role in the urban heat island effect and different blocks and landscape types have different temperature change characteristics (Yue et al. 2013; Coseo and Larsen 2014; Wang et al. 2017; Yang et al., 2019b; Manob and Arijit 2020; Qiao et al. 2020). The density and area of land cover types affect LST. Some land cover types can reduce urban LST by 1.4–6.1 °C, such as green spaces and water bodies (He et al., 2019; Park et al. 2019; Wu et al. 2019a; Guo et al. 2020; Jamshid et al. 2020). Under undisturbed weather conditions, the temperature of the artificial LCZ is significantly higher than that of the land cover LCZ (Oke 1982; Beck et al. 2018). Thus, comparing of the thermal environment in cities of different sizes, it is seen that the temperature of different LCZs has certain common characteristics.

Research on the thermal environment of LCZs mainly considers a single city or street community as the study scale and thus lacks a regional scale. Our study aims to investigate the LCZs temperature hierarchy effect of different sized cities in urban agglomerations on the regional scale. LCZ types are divided based on certain parameters, LST is inverted by a mono-window algorithm, and overlay analysis is used to obtain the temperatures of various LCZs in cities of different sizes. LCZs can spatially exhibit the interaction among urban climatic conditions, surface structure, and land use (Chen and Tang 2017). Thus, comparing the thermal environmental differences of various LCZs in cities of different sizes is helpful to identify the thermal environment management needs of different cities. This could help reduce urban energy consumption, improve local climate, and alleviate the urban heat island effect. We hope that our research can provide scientific insights for thermal environment management and urban climate improvement in the Pearl River Delta urban agglomeration.

2. Materials and methods

2.1. Study area

The Pearl River Delta urban agglomeration is located in the southeast of Guangdong Province (111°59′–115°28′ E, 21°30′–23°40′ N), in the lower reaches of the Pearl River and is characterized by flat terrain (Fig. 1). The Pearl River Delta, located on and south of the Tropic of Cancer, has a subtropical monsoon climate, being warm and humid throughout the year, with a mean annual temperature of 21–23 °C. The delta is affected by typhoons from June–October, with concentrated rainfall and the highest temperatures. In 2015, the Pearl River Delta urban agglomeration became the urban agglomeration with the largest population and area in the world, where high urbanization resulted in significant local climate change (World Bank Group 2015). Therefore, the present study selected the eight cities of Guangzhou, Shenzhen, Dongguan, Foshan, Huizhou, Jiangmen, Zhongshan, and Zhuhai in the Pearl River Delta urban agglomeration as the study area for the examination of temperature differences among LCZs in cities of different sizes.

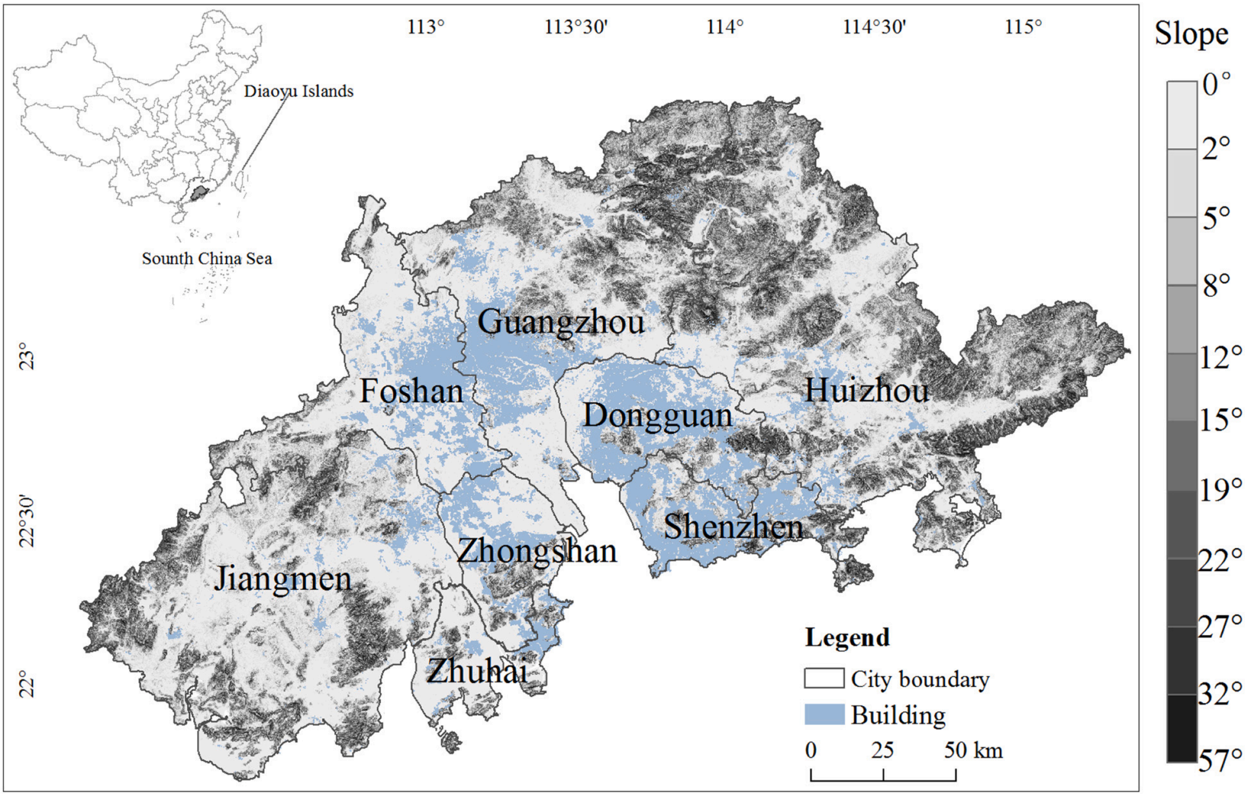

Fig. 1. Location of the urban agglomeration of Pearl river delta.

Table 1
Explanation of data used in this study.

	Resolution	Data time	Data source	Sample
Landsat8 OLI/TIRS	30 m	2015-01-19;2016-02-07; 2018-01-18;2018-02-03; 2018-02-12;2018-03-09; 2019-01-23	http://www.usgs.gov	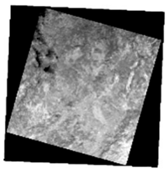
Land use data	100 m	2015	http://www.resdc.cn	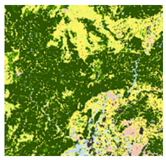
Building data	30 m	2016	https://map.baidu.com	
Meteorological data	–	2015-01-19;2016-02-07; 2018-01-18;2018-02-03; 2018-02-12;2018-03-09; 2019-01-23	https://rp5.cu	–

Table 2
Classification of city hierarchy.

City size	City	Permanent residents(million)
Super city (permanent residents ≥ 10^7)	Shenzhen	13.03
	Guangzhou	12.87
Megacity ($5.0*10^6 \leq$ permanent residents < 10^7)	Dongguan	7.64
	Foshan	7.51
Type I large city ($3.0*10^6 \leq$ permanent residents < $5.0*10^6$)	Huizhou	3.39
Type II large city ($10^6 \leq$ Permanent residents < $3.0*10^6$)	Jiangmen	3.06
	Zhongshan	2.92
	Zhuhai	1.70

2.2. Data

The research data of the present study included Landsat 8 OLI/TIRS, land use, building, and meteorological data (Table 1). Because the climate of the study area is cloudy and rainy, and the area is large, obtaining remote sensing images that can meet the cloud cover requirements of LST inversion is difficult. Therefore, Landsat 8 data during seven time periods in the first quarter of different years were selected. The reasons for selecting data from these periods were as follows: 1) they had more sunny weather with less cloud cover in the first quarter and 2) an attempt was made to pick a date that was close to the land use data and building data. The remote sensing data was then processed in ENVI using the FLAASH atmospheric correction module to eliminate the influence of the atmosphere and sun on the reflection information. Simultaneously, the land-use raster data and building vector data in 2015 were regarded as the supporting data for the division of LCZs. Although the resolution of land use data was lower than that of building data, the present study employed ArcGIS resample tools to ensure that the land-use data raster cell size matched the building data.

2.3. Methods

2.3.1. Classification of city size

In our study, cities were classified according to the new city size classification standard issued by China (RPC, 2014), and were divided into four sizes according to the permanent resident population in the study area: super cities—Guangzhou and Shenzhen; megacities—Dongguan and Foshan; type I large cities—Huizhou and Jiangmen, and type II large cities—Zhongshan and Zhuhai (Table 2).

2.3.2. LST retrieval

Remote sensing image of the first quarter was used as inversion data is because ofthe rainfall in our study area; the atmospheric stability promotes the best accuracy of remote sensing and at the same time aggravates the effect of urban heat islands. The Qin Zhihao mono-window algorithm was applied to retrieve LSTs (Qin et al. 2001; Wang et al. 2015), from which the surface thermal radiation transfer equation was derived. Landsat thermal infrared band 10 was used to retrieve the LST through the following formulas:

$$T_S = [a(1 - C - D) + (b(1 - C - D) + C + D)T_{\text{sensor}} - DT_a]/C] \tag{1}$$

$$C = \tau\varepsilon \tag{2}$$

$$D = (1 - \tau)[1 + (1 - \varepsilon)\tau] \tag{3}$$

where ε is the surface emissivity; τ is the atmospheric transmittance; T_{sensor} is the brightness temperature corresponding to the onboard radiance; T_S is the retrieved LST; T_a is the average atmospheric temperature; a and b are coefficients, whose values were −67.35535 and 0.45861, respectively, and; C and D were intermediate quantities calculated by formulas (2) and (3).

2.3.3. LCZs classification

The LCZ classification system divides LCZs into two major categories: built LCZ and land cover LCZ (Fig. 2). Therefore, according to the actual situation of cities in the Pearl River Delta urban agglomeration, we classify built LCZ into seven categories (LCZ 1–7) and categorize the buildings as low, medium, and high according to three interval values (3–9 m, 9–27 m, and over 27 m). The building density is divided into open and compact. The land cover LCZ is classified into seven types (LCZ A- G) according to the sparse and dense types of surface coverage in the Pearl River Delta urban agglomeration. After setting the classification standards, the industrial building is separated from the non-industrial building according to the building attributes. Using non-industrial building data to divide LCZ 1–6 requires calculation of average building height and average building density. The average building height is reclassified into three categories: high, medium and low. The average building density is reclassified into two categories: compact and open. We cross-calculated the two reclassification results to obtain the non-industrial building LCZ classification results (i.e., LCZ 1-LCZ 6) and industrial building data are regarded as LCZ 7. Meanwhile, the land cover LCZ combines the classification standards in order to qualitatively divide the land use data to obtain LCZ A- G. After the LCZ classification results are obtained, they can be combined with LST, and the temperature of different types of LCZ can be obtained by overlay analysis.

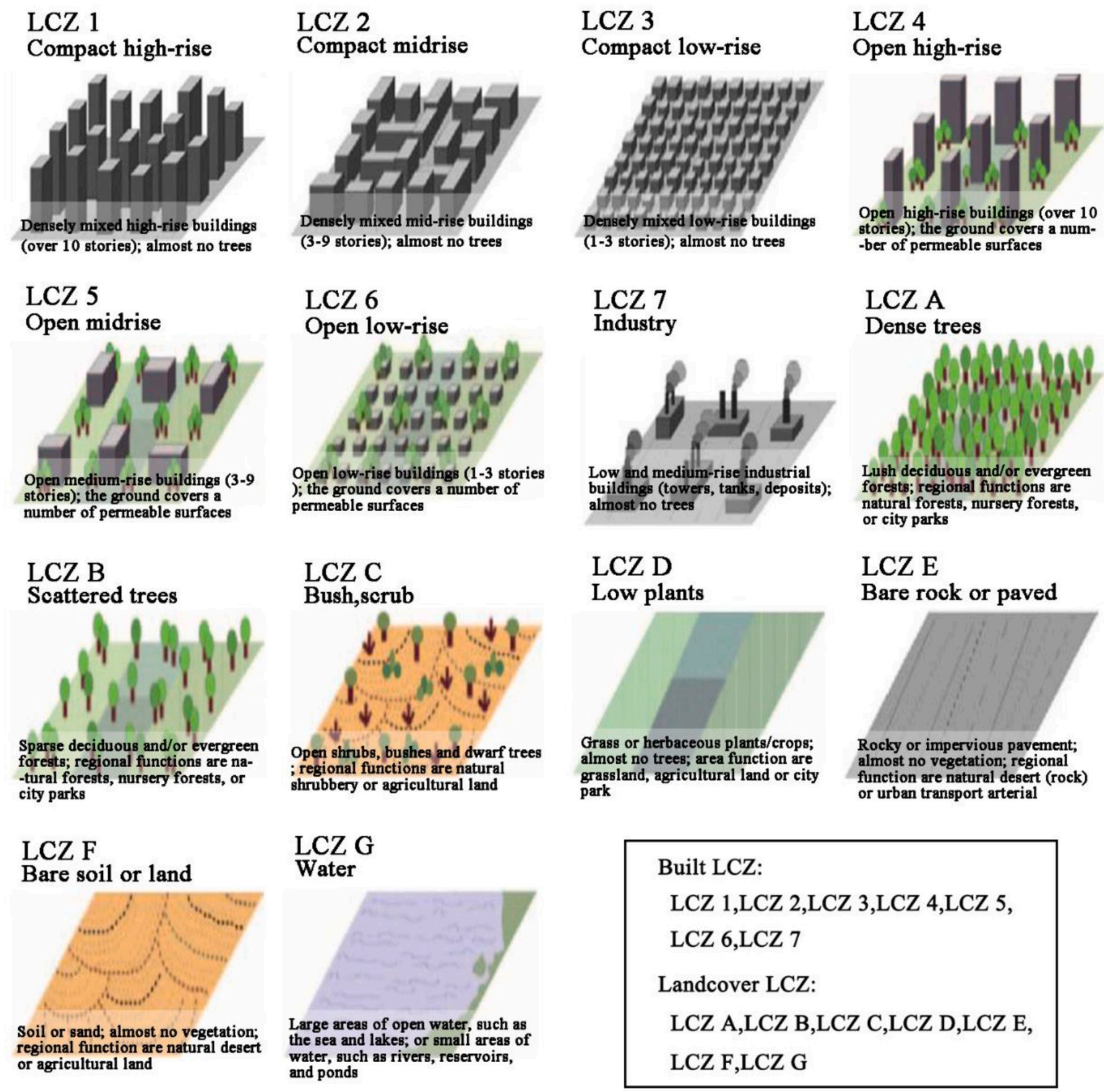

Fig. 2. Classification of local climate zones and description of their definitions (Referenced: Timothy R Oke).

3. Results

3.1. LST in cities of different sizes

In the Pearl River Delta urban agglomeration, the relief was high in the east and west and low in the center (Fig. 1). The orientation of the relief affects LST because the shaded side is less exposed to the sun's rays and the LST is thus low. In our study area, areas with high LST had low relief slopes and many buildings, and areas with low LST were mainly concentrated in the study areas with high relief slope. Thus, the LST in cities showed a tendency of gathering in one or more centers, which was more obvious in larger cities (Fig. 3). We defined the area where LST was higher than 20 °C as the high temperature area. Shenzhen has a large number of buildings with the LST of most areas being higher than 18 °C. The high temperature areas were mainly located in the northwest, the low LST area was concentrated in the southeast area with high relief slope, and the northwest side of the relief slope received less sunlight. In Guangzhou, the high temperature areas were mainly located in the southwest where many buildings exist, and the LST in the northeast region was lower than 16 °C with high relief slope. Like Shenzhen, Dongguan's buildings were widely distributed, where the LST in most areas was between 18 and 38 °C, and the low temperature areas were mainly located in the

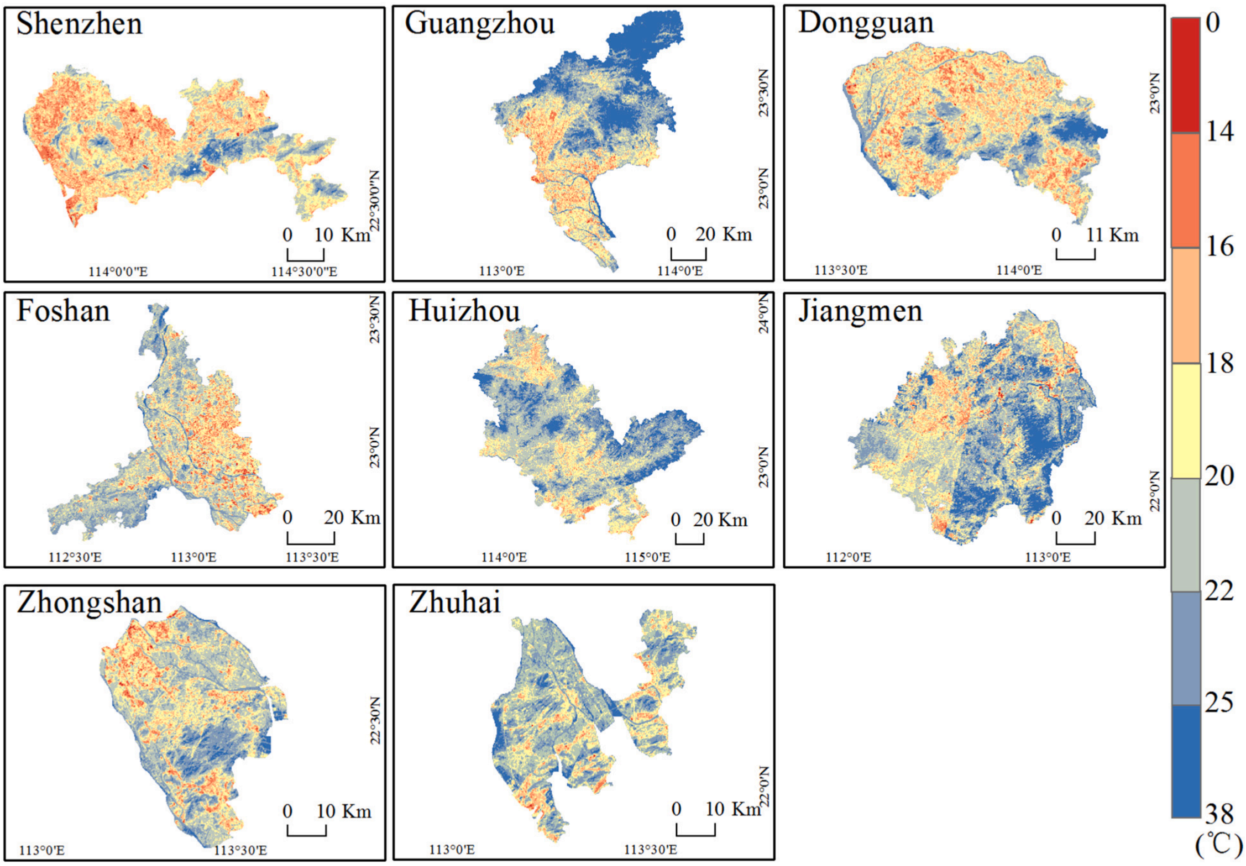

Fig. 3. Results of land surface temperature inversion for each city.

southeast area with high relief slope. In most areas of Foshan, the LST was higher than 18 °C, and the high temperature areas were mainly located in the east and south with the amount of buildings. The areas with high LST in Huizhou were concentrated in the southwest and northwest, whereas the concentration of the high temperature areas in Jiangmen decreased, mainly in the northwest and northeast. Huizhou and Jiangmen have more areas with LST below 16 °C compared with super cities and megacities, owing to relatively fewer buildings and the high slope of the relief, and the Landsat 8 satellites acquired land information between approximately between 10:45 and 11: 00 am China Standard Time. The northwest and northeast side of the relief were less exposed to sunrays, and thus the LST was low. The high temperature areas in Zhongshan were prevalent in the northwest; however, a small number of high temperature areas were located in areas with a high slope of the relief. Zhuhai's overall relief slope is relatively low, and high temperature areas were scattered and the number was less than in larger cities. The locations of high temperature areas were mainly affected by the distribution of buildings.

3.2. LCZ classification of different sizes of cities

As shown in Fig. 4 and Tables 3 and 4, among the super cities, built LCZs in Shenzhen were concentrated and large in area, among which LCZ 5 had the largest proportion, accounting for 35.17%. There were many LCZ E near LCZ 1; however, there were no land cover LCZs between built LCZs. In land cover LCZs, the number of LCZ E was the largest, accounting for 48.78%, whereas the land cover type was dominated by LCZ A. Guangzhou had a large urban area; however, its built LCZ were concentrated along the Pearl River and in the vicinity of estuaries. Among the built LCZs in Guangzhou, the number of LCZ 6 was the largest, accounting for 31.79%. Unlike Shenzhen, Guangzhou had a small proportion of LCZ 1 but a large proportion of LCZ 3; LCZ E accounted for only 19.98%. However, there were many examples of LCZ A and LCZ D. Among megacities, the dense buildings in Dongguan were clustered and distributed in patches. LCZ 2 accounted for 19.35% of the built LCZ in the city, and the number was almost twice that of megacities. However, the proportion of LCZ 1 was only 1.34%. The situation in Dongguan was the same as in Shenzhen. The proportion of LCZ E in land cover LCZ was higher than 40%; however, there were fewer LCZ A. Built LCZ in Foshan were primarily distributed in the area bordering Guangzhou. Among them, LCZ 6 had the largest number, accounting for 40.40%, and LCZ 3 accounted for 21.94%, both of which outnumbered those in super cities. However, the proportion of LCZ 1 in Foshan was the smallest in the entire study area. Among land cover LCZ in Foshan, the number of LCZ D was higher than that of LCZ A, accounting for 33.62%, while LCZ E accounted for 31.05%.

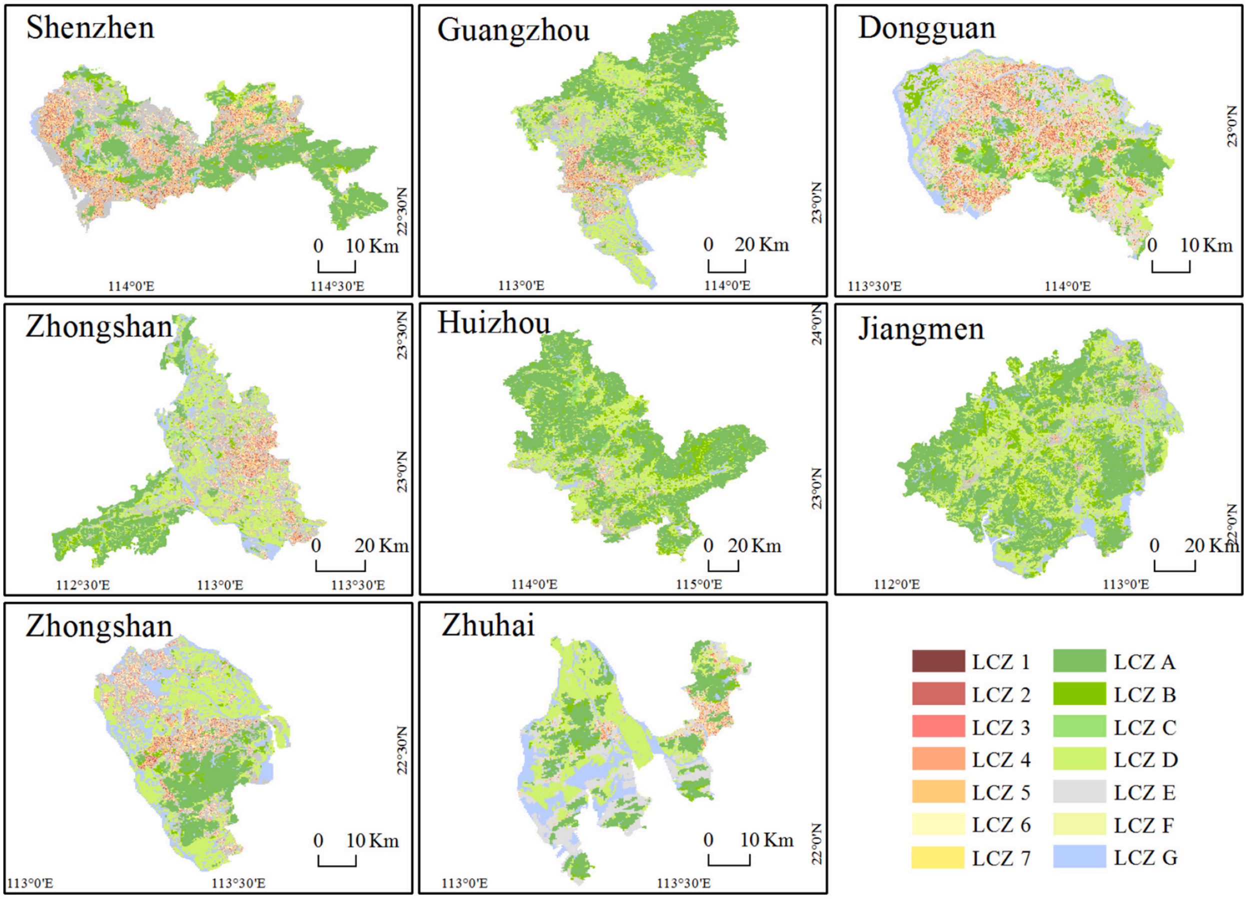

Fig. 4. Classification map of local climate zones in the study area: a) Shenzhen, b) Guangzhou, c) Dongguan, d) Foshan, e) Huizhou, f) Jiangmen, g) Zhongshan, h) Zhuhai.

Table 3
Percentage of various types of built LCZ in different size cities.

City size		Super city		Megacity		Type I large city		Type II large city	
City		Shenzhen	Guangzhou	Dongguan	Foshan	Huizhou	Jiangmen	Zhongshan	Zhuhai
Built LCZ	LCZ 1	3.74%	2.75%	1.34%	1.09%	1.25%	3.76%	1.49%	2.36%
	LCZ 2	12.94%	12.13%	19.35%	8.53%	2.64%	3.35%	9.19%	9.67%
	LCZ 3	6.74%	10.57%	10.08%	21.94%	14.02%	10.33%	18.67%	7.02%
	LCZ 4	11.52%	9.62%	4.21%	3.97%	5.87%	18.26%	4.53%	10.85%
	LCZ 5	35.17%	31.11%	37.39%	16.24%	12.82%	16.46%	19.53%	34.92%
	LCZ 6	28.61%	31.79%	26.64%	40.40%	63.36%	46.73%	40.32%	27.54%
	LCZ 7	1.28%	2.03%	0.99%	7.83%	0.05%	1.11%	6.27%	7.65%

In the type I large cities of Huizhou and Jiangmen, built LCZs were fewer and more scattered, with LCZ 1 amounting to half of those in megacities. In Huizhou, LCZ 6 accounted for 63.36%, which was the largest. LCZ E contributed only 6.85% of the land cover LCZ in the city, whereas LCZ A accounted for 53.24%, with the area of land cover greatly outnumbering that in super cities and megacities. LCZ A and LCZ D were the principal land cover LCZ. In Jiangmen, the proportions of LCZ 4 and LCZ 5 were higher than those in Huizhou at the same size; however, there were fewer LCZ 3. The numbers of LCZ A, LCZ B, and LCZ D in land cover LCZs were higher than those in super cities and megacities. In the type II large city of Zhongshan, LCZ 6 was the primary built LCZ, accounting for 40.32%, combined with the proportion of LCZ E being almost the same as that in megacities, and LCZ D representing 31.72% of the land cover LCZ. Zhuhai was the smallest size city, where the total number of built LCZ was the least among the cities in the study area. The built LCZ in the city were dominated by LCZ 5 (accounting for 34.92%), and LCZ A, LCZ G, and LCZ E accounted for higher than 20% of land cover LCZ.

Table 4
Percentage of various types of land cover LCZ in different size cities.

City scale		Super city		Megacity		TypeIlarge city		TypeIIlarge city	
City		Shenzhen	Guangzhou	Dongguan	Foshan	Huizhou	Jiangmen	Zhongshan	Zhuhai
Land cover LCZ	LCZ A	34.50%	36.10%	13.28%	17.06%	53.24%	38.99%	17.45%	24.08%
	LCZ B	3.73%	5.18%	9.07%	4.45%	9.52%	10.01%	2.50%	2.07%
	LCZ C	0.74%	1.77%	0.58%	0.58%	1.29%	0.45%	–	0.07%
	LCZ D	9.07%	30.14%	14.91%	33.62%	26.00%	32.88%	31.72%	29.04%
	LCZ E	48.78%	19.98%	49.98%	31.05%	6.85%	8.78%	30.12%	26.47%
	LCZ F	–	0.03%	0.01%	0.05%	0.02%	0.01%	0.02%	0.24%
	LCZ G	3.17%	6.79%	12.17%	13.19%	3.08%	8.88%	18.20%	18.03%

3.3. LCZ temperature in different sizes of cities

Differences were observed in the mean temperatures of various LCZ types. Among built LCZ, the mean temperature of LCZ 7 was the highest (21.810 °C), followed by that of LCZ 3 (20.953 °C), LCZ 2 (20.367 °C), LCZ 6 (20.292 °C), LCZ 5 (19.948 °C), and LCZ 4 (the lowest at 19.136 °C). The mean temperatures of built LCZ in the cities in the study area from high to low were: LCZ 7 > LCZ 3 > LCZ 2 > LCZ 6 > LCZ 5 > LCZ 1 > LCZ 4 (Fig. 5). In land cover LCZ, the mean temperature of LCZ E was the highest (19.262 °C), followed by that of LCZ D (17.757 °C), LCZ F (17.442 °C), LCZ B (17.336 °C), LCZ C (17.027 °C), LCZ G (16.518 °C), and LCZ A (the lowest at 15.670 °C). The overall trend in the mean temperatures of land cover LCZ from high to low was: LCZ E > LCZ D > LCZ F > LCZ B > LCZ C > LCZ G > LCZ A.

As shown in Tables 3 and 4, land cover LCZ with a temperature that was higher than 20 °C were scarce, and low-temperature land cover LCZ accounted for a large proportion of the urban land surface. In the super city of Shenzhen, a built LCZ was observed, among which midrise and low-rise buildings of LCZ 2, LCZ 5, LCZ 6 with high temperature accounted for a significant proportion. In terms of land cover LCZ, the proportion of LCZ E with a mean temperature of 20.505 °C reached 48.78%; that of LCZ A with a mean temperature of 17.432 °C reached 34.50%, and that of other land cover types with low temperatures contributed less than 10%. In Guangzhou, although the proportion of LCZ 5 and LCZ 6 exceeded 30%, the proportion of LCZ A with a mean temperature of 13.089 °C reached 36.10%, that of LCZ E with high mean temperature was only 19.98%, and that of LCZ G with a mean temperature of 16.528 °C was 6.79%. The temperatures of all LCZ types in Guangzhou were significantly lower than those in Shenzhen (Fig. 5 a and b). In megacities, LCZ 5 with a mean temperature of 20.449 °C in Dongguan accounted for 37.39%, and LCZ 6 with a mean temperature of 20.682 °C in Foshan accounted for 40.40%. Although the proportion of LCZ A with low mean temperatures in the two cities was small, there were several of LCZ E. Moreover, LCZ G accounted for 12.17% of natural areas in Dongguan and 13.19% in Foshan, and the proportion of LCZ B was also higher than that in Shenzhen. In the type I large city Huizhou, the proportion of all built LCZ except LCZ 6 (mean temperature: 18.585 °C) was lower than 15%. LCZ A with a mean temperature of 15.756 °C, accounted for 53.24% of land cover LCZ, whereas LCZ E with a mean temperature of 19.124 °C, accounted for only 6.85%. The mean temperature of the built LCZ in Jiangmen was higher than that in Huizhou. In Jiangmen, LCZ 6 (mean temperature: 21.488 °C) accounted for 46.73% of built LCZ, LCZ D (mean temperature: 17.703 °C) accounted for 32.88%, and LCZ E (mean temperature: 19.024 °C) accounted for 8.78%, which was higher than that in Huizhou. In the type II large cities of Zhongshan and Zhuhai, the total number of buildings was much lower than those in super cities and megacities. The proportions of LCZ D and LCZ E with higher temperatures were higher than 25%. However, LCZ A in Zhongshan (mean temperature: 15.851 °C) accounted for 17.45%, in Zhuhai (mean temperature: 16.358 °C) it accounted for 24.08%, and this proportion was higher than 18% of LCZ G with low mean temperatures in both cities.

There was a significant temperature hierarchy effect among LCZs in cities of different sizes (Fig. 6). In relatively larger cities, the temperatures of all LCZs were high (Fig. 5). The highest LCZs temperature was 20.841 °C in super cities (i.e., 0.328 °C higher than that in megacities), 20.513 °C in megacities (0.323 °C higher than that in type I large cities), and 20.190 °C in type I large cities (0.546 °C higher than that in type II large cities at 19.622 °C). The temperature difference between LCZs in megacities and type I large cities was the smallest, whereas that between LCZs in type II large cities and super cities was the largest. Consequently, in the Pearl River Delta urban agglomeration, there was a hierarchy effect of LCZs temperature in cities of different sizes, in the following order: super cities > megacities > type I large cities > type II large cities.

4. Discussion

From the results of our study (Fig. 5), it can be concluded that large cities have large numbers of compact buildings: compact midrise (LCZ 2) and high-rise buildings (LCZ 1) are widely distributed, with less land cover LCZ and small water areas (LCZ G). In contrast, buildings in smaller cities mainly comprise low-rise and medium-rise buildings. However, the number of built LCZs is less than that of larger size cities, with more land cover LCZs and wide water areas (LCZ G). Vegetation and water bodies are critical factors in regulating local climate (Feyisa et al., 2014; Du et al. 2019; Wang et al. 2019). Under normal temperature conditions, for every 10% increase in canopy percentage, the LST decreases by 0.2 °C, whereas for every 10% increase in impervious surface area, the LST in the urban area increases by 0.7 °C (Klok et al. 2012; Wu et al., 2019a, b). The Pearl River Delta region has a developed economy, dense population, and a high degree of urbanization. All cities in the study area are at least large-sized cities, the proportion

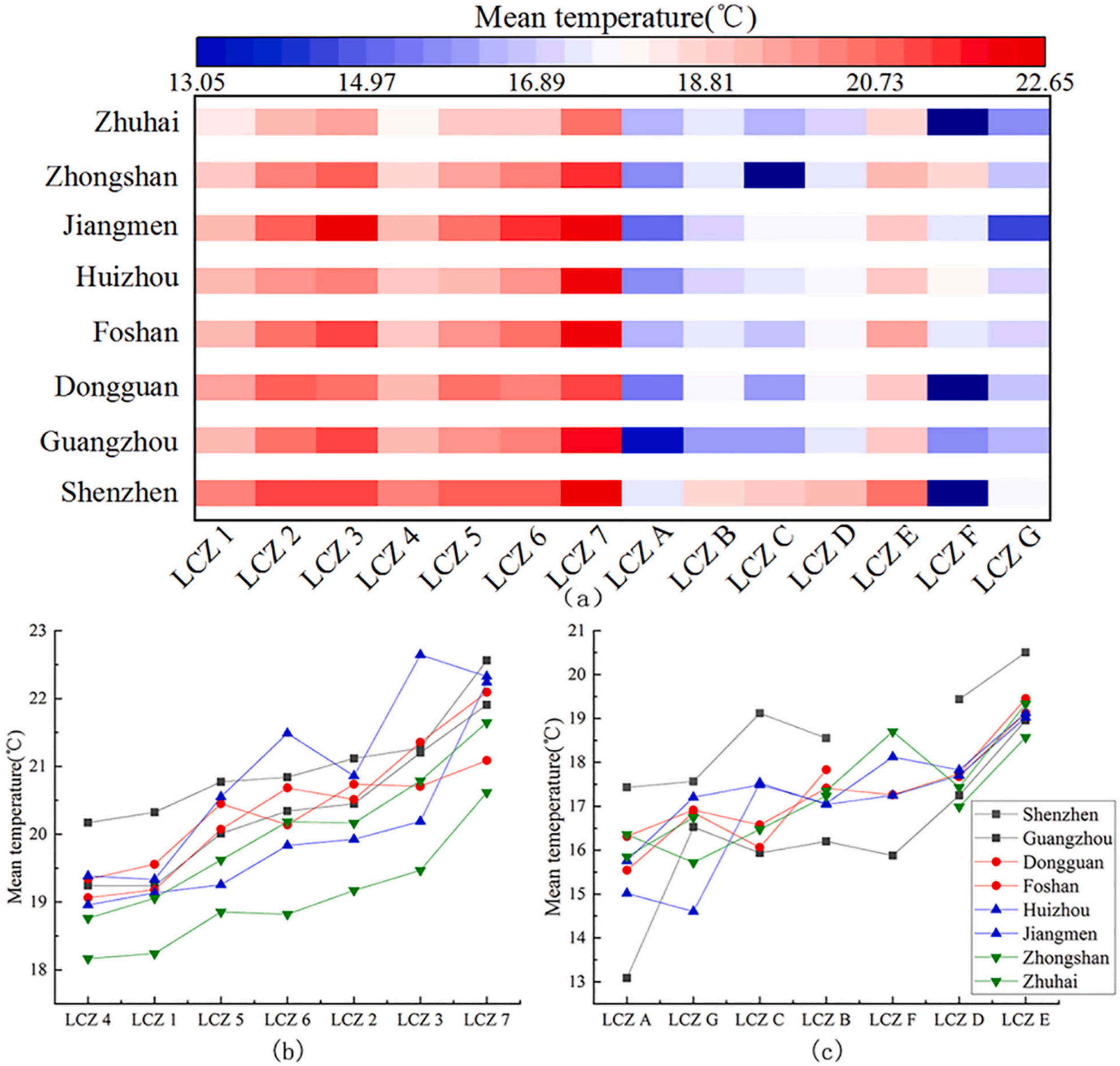

Fig. 5. LCZs temperatures in different size cities:a) Heat map of LCZs, b) temperature of land cover LCZ (Cities of the same size are represented by the same color), c) temperature of built LCZ (Cities of the same size are represented by the same color).

of bare rock or paved areas (LCZ E) in each city is large, and the vegetation in urban greening is dominated by dense trees (LCZ A) and low plants (LCZ D). In our study area, super cities and megacities have large populations, heavy traffic, and busy living trends, which readily generate large amounts of waste heat. Furthermore, as is typical in large-sized cities, there are many dense mid-rise and low-rise buildings (LCZ 2 and LCZ 3), and there exists extensive coverage of impervious pavements (LCZ E, especially in Shenzhen and Dongguan), and low coverage of vegetation and water conducive to cooling the urban area. Thus, megacities have the highest temperatures and are subject to significant urban heat island effects (Fig. 6).

In Chapter 1, we mention that the current research on LCZs is mainly focused on the perspective of the meso-microscale. In contrast, our study examined the temperature hierarchy effect of LCZs in cities of different sizes in urban agglomerations on the regional scale. This differs from the approach taken in previous LCZs studies, and more reliable conclusions can be drawn by comparing multiple samples as is done in our study. Furthermore, although LCZ mapping methods have gradually improved, the accuracy of final algorithmic identification results of LCZs are yet to be verified by field investigations or remote sensing experts to allow for visual interpretation. However, we used high-resolution vector data combined with raster data to classify LCZs in our study. The addition of vector data could improve the classification accuracy of LCZs and enhance the accuracy of the classification results (Huang et al. 2007; Lelovics et al. 2013; Huang et al. 2014).

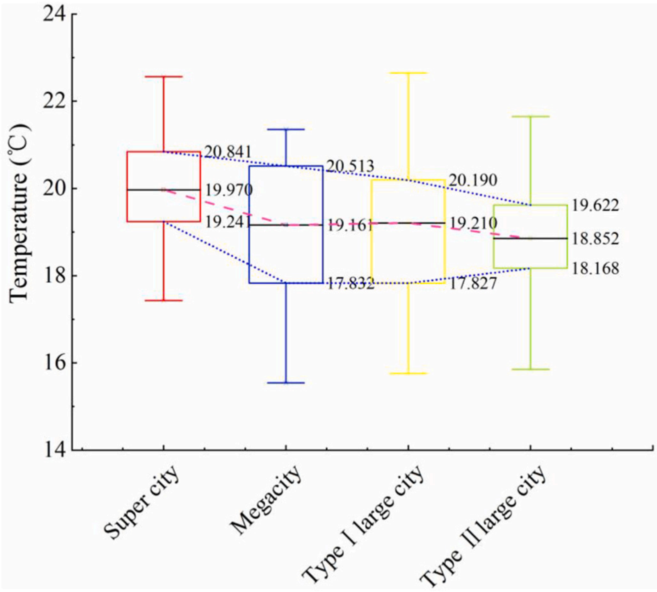

Fig. 6. The hierarchy effect of LCZs land surface temperature in different size cities. Super city: Shenzhen, Guangzhou; Megacity: Dongguan, Foshan; TypeIlarge city: Huizhou, Jiangmen; Type II large city: Zhongshan, Zhuhai.

However, there were some limitations in our study. Due to the large study area and cloudy and rainy weather, Landsat 8 images in the first quarter of different years were selected as temperature retrieval data to ensure that remote sensing images were not affected by cloud cover, which influenced LST retrieval results to a certain extent. Although our results proved that there were differences in the LCZs' temperature among cities of different sizes, there are many uncontrollable factors in regional-scale research and further research is required to evaluate their impact. Moreover, some buildings, such as temporary buildings, were not included in our study.

5. Conclusion

We used building vector data and satellite raster images to perform LCZs classification, conduct overlay analysis of the classification results and the LST results, quantify the LCZs' temperature of cities of different sizes, and determine the LCZs temperatures of cities of different sizes in rank order. We obtained the following conclusions:

1) The distribution of buildings and the relief slope affects LST. In the Pearl River Delta urban agglomeration, there are few to no buildings in areas with LST lower than 14 °C, but areas with a large number of buildings are usually accompanied by high LST, and areas with high relief slope usually have low LST. Larger cities have more buildings, and thus there were more areas with LST over 18 °C than the smaller size cities.
2) The density, quantity, and properties of LCZs are different, and hence their temperature is different. The overall temperature variation trend of land cover LCZ was: LCZ E > LCZ D > LCZ F > LCZ B > LCZ C > LCZ G > LCZ A. Among them, the mean temperature of LCZ A (dense trees) was the lowest (15.670 °C), whereas that of LCZ E (bare rock or pavement) was the highest (19.262 °C). LCZ E will increase LST, but LCZ A and LCZ G can cool LST. The overall temperature variation trend of built LCZ was: LCZ 7 > LCZ 3 > LCZ 2 > LCZ 6 > LCZ 5 > LCZ 1 > LCZ 4. The mean temperature of LCZ 7 (industry) was the highest (21.810 °C) whereas that of LCZ 4 (open high-rise) was the lowest (19.136 °C).
3) Compared with smaller sized cities, larger cities had more built LCZs, which exhibited higher temperatures. LCZ 2, LCZ 3, LCZ 5, and LCZ 6 temperature results show that the larger the city, the higher the LCZs temperature, i.e., super cities > megacities > type I large cities > type II large cities. Therefore, the temperature of LCZs among cities of different sizes has a hierarchy effect.
4) The mean temperature of mid-rise and low-rise buildings (such as LCZ 2, LCZ 3, LCZ 5, and LCZ 6) were higher than that of high-rise buildings such as LCZ 1, indicating that the building height has little effect on the LST of a built LCZ.

In conclusion, by exploring the differences in LCZs temperature among cities of different sizes, the present study determined the differences between the thermal environments of different land features. Cities of different sizes have different environmental requirements, and thus an effective basis for the cities to implement thermal environment management, according to the local conditions, is provided. In the Pearl River Delta urban agglomeration, for super cities and megacities with high LCZ temperatures, promoting the organization of LCZ A and LCZ G during urban planning, and reducing the number of LCZ E while reducing building density, to enhance the urban ventilation capacity is necessary. For type I and type II large cities, it is essential to reduce the number of mid-rise and low-rise buildings, increase the number of high-rise buildings, and improve the rationality of building distribution. Furthermore, the impact of industrial heat on urban life should be minimized, modification of industrial structure should be promoted, and factories should be transformed for environmental protection purposes. The LCZs should be reasonably organized according to the actual environment needs of cities. For cities with many dense buildings, setting proper building density is required. LCZs which are conducive to lowering the temperature of urban spaces should be increased, and the location and size of LCZs appropriately adjusted to regulate local climate. This could effectively reduce the urban heat island effect and also provide a reference for urban agglomerations in other areas.

Declaration of Competing Interest

This manuscript has not been published or presented elsewhere in part or in entirety and is not under consideration by another journal. We have read and understood your journal's policies, and we believe that neither the manuscript nor the study violates any of these. There are no conflicts of interest to declare.

Acknowledgments

This research study was supported by the National Natural Science Foundation of China (grant no. 41771178, 41630749, 41471140) and Liaoning Province Innovative Talents Support Program (Grant No. LR2017017). The authors would like to thank all experts for their contributions to the urban thermal environment and urban planning.

References

Albert, C., Schröter, B., Haase, D., Brillinger, M., Henze, J., Herrmann, S., et al., 2019. Addressing societal challenges through nature-based solutions: how can landscape planning and governance research contribute. Landsc. Urban Plan. 182, 12–21. https://doi.org/10.1016/j.landurbplan.2018.10.003.
Bechtel, B., Alexander, J. P., Böhner, J., JasonChing, Conrad, O. & Feddema, J. et al. (2015). Mapping local climate zones for a worldwide database of the form and function of cities. ISPRS Int. J. Geo.Inform., 4(1), 199–219. doi:https://doi.org/10.3390/ijgi4010199.
Beck, C., Straub, A., Breitner, S., Cyrys, J., Philipp, A., Rathmann, J., et al., 2018. Air temperature characteristics of local climate zones in the Augsburg urban area (Bavaria, southern Germany) under varying synoptic conditions. Urban Clim. 25, 152–166. https://doi.org/10.1016/j.uclim.2018.04.007.
Brousse, O., Georganos, S., Demuzere, M., Vanhuysse, S., Wouters, H., Wolff, E., et al., 2019. Using local climate zones in sub-Saharan Africa to tackle urban health issues. Urban Clim. 27, 227–242. https://doi.org/10.1016/j.uclim.2018.12.004.
Cai, M., Ren, C., Xu, Y., Dai, W., Wang, X.M., 2016. Local climate zone study for sustainable megacities development by using improved WUDAPT methodology –a case study in Guangzhou. Procedia Environ. Sci. 36, 82–89. https://doi.org/10.1016/j.proenv.2016.09.017.
Chen, K., Tang, Y., 2017. Research progress of urban local climate zone and its application in urban planning. South Archit. 02, 21–28.
Chen, Y.C., Lin, P.T., Wan, Y.S., 2017. Modeling the urban thermal environment distributions in Taipei Basin using Local climate zone (LCZ). Joint Urban Remote Sensing Event (JURSE).
Coseo, P., Larsen, L., 2014. How factors of land use/land cover, building configuration, and adjacent heat sources and sinks explain urban Heat Islands in Chicago. Landsc. Urban Plan. 125, 117–129. https://doi.org/10.1016/j.landurbplan.2014.02.019.
Cui, L.L., Shi, J., 2012. Urbanization and its environmental effects in Shanghai, China. Urban Clim. 2, 1–15. https://doi.org/10.1016/j.uclim.2012.10.008.
Danylo, O., See, L., Bechtel, B., Schepaschenko, D., Fritz, S., 2016. Contributing to WUDAPT: a local climate zone classification of two cities in Ukraine. IEEE J. Select. Topics Appl. Earth Observ. Remote Sens. 9 (5), 1841–1853. https://doi.org/10.1109/JSTARS.2016.2539977.
Du, J., Song, K.S., Yan, B.H., 2019. Impact of the Zhalong wetland on Neighboring land surface temperature based on remote sensing and GIS. Chin. Geogr. Sci. 29 (5), 798–808. https://doi.org/10.1007/s11769-019-1050-2.
Emmanuel, M.O., Elham, F., Aggrey, O.A., John, B.M., John, M.W., Sahar, S., 2020. Inter-local climate zone differentiation of land surface temperatures for management of Urban Heat in Nairobi City, Kenya. Urban Clim. 31, 100540. https://doi.org/10.1016/j.uclim.2019.100540.
Fang, J.Y., Yu, G.R., Liu, L.L., Hu, S.J., Chapin, F.S., 2018. Climate change, human impacts, and carbon sequestration in China. Proc. Natl. Acad. Sci. 115 (16), 4015–4020. https://doi.org/10.1073/pnas.1700304115.
Feyisa, G.L., Dons, K., Meilby, H., 2014. Efficiency of parks in mitigating urban heat island effect: an example from Addis Ababa. Landsc. Urban Plan. 123, 87–95. https://doi.org/10.1016/j.landurbplan.2013.12.008.
Franco, M.P.D., Andrade, D.F.M., Yuri, Y.R., Ching, J., 2019. Effect of local climate zone (LCZ) classification on ozone chemical transport model simulations in Sao Paulo, Brazil. Urban Clim. 27, 293–313. https://doi.org/10.1016/j.uclim.2018.12.007.
Guo, A.D., Yang, J., Xiao, X.M., Xia, J.C., Jin, C., Li, X.M., 2020. Influences of urban spatial form on urban heat island effects at the community level in China. Sustain. Cities Soc. 53, 101972. https://doi.org/10.1016/j.scs.2019.101972.
He, B.J., Zhao, Z.Q., Shen, Du, Wang, Li, B, H., Li, L.G., 2019. An approach to examining performances of cool/hot sources in mitigating/enhancing land surface temperature under different temperature backgrounds based on Landsat 8 image. Sustain. Cities Soc. 44, 416–427. https://doi.org/10.1016/j.scs.2018.10.049.
Hong, C.P., Zhang, Q., Zhang, Y., Davis, J.S., Tong, D., Zheng, Y.X., et al., 2019. Impacts of climate change on future air quality and human health in China. Proc. Natl. Acad. Sci. 116 (35), 17193–17200. https://doi.org/10.1073/pnas.1812881116.
Huang, X., Zhang, L.P., Li, P.X., 2007. Classification and extraction of spatial features in urban areas using high-resolution multispectral imagery. IEEE Geosci. Remote Sens. Lett. 4 (2), 260–264. https://doi.org/10.1109/LGRS.2006.890540.
Huang, X., Lu, Q.K., Zhang, L.P., 2014. A multi-index learning approach for classification of high-resolution remotely sensed images over urban areas. ISPRS J. Photogramm. Remote Sens. 90, 36–48. https://doi.org/10.1016/j.isprsjprs.2014.01.008.
Jamshid, D., Shahram, P.D., Valentina, D., Mohammad, R.H., Morteza, A., 2020. The impact of green space structure on physiological equivalent temperature index in open space. Urban Clim. 31, 100574. https://doi.org/10.1016/j.uclim.2019.100574.
Jan, G., Michal, L., Stevan, S., Dragan, M., 2018. Modelled spatiotemporal variability of outdoor thermal comfort in local climate zones of the city of Brno, Czech Republic. Sci. Total Environ. 624, 385–395. https://doi.org/10.1016/j.scitotenv.2017.12.076.
Kang, K.Y., 2013. Urban form and residential energy use: a review of design principles and research findings. J. Plan. Lit. 28 (4), 327–351. https://doi.org/10.1177/0885412213491499.
Klok, L., Zwart, S., Verhagen, H., Mauri, E., 2012. The surface heat island of Rotterdam and its relationship with urban surface characteristics. Resour. Conserv. Recycl. 64, 23–29. https://doi.org/10.1016/j.resconrec.2012.01.009.
Kotharkar, R., Bagade, A., 2017. Local climate zone classification for Indian cities: a case study of Nagpur. Urban Clim. 24, 369–392. https://doi.org/10.1016/j.uclim.2017.03.003.
Lelovics, E., Unger, J., Gal, T., 2013. Mapping Local Climate Zones with a Vector-Based GIS Method. Aerul Şi Apa Componente Ale Mediului. pp. 230–423.
Lelovics, E., Unger, J., Gal, T., 2014. Designation of an urban monitoring network based on local climate zone mapping and temperature pattern modelling. Clim. Res. 60 (1), 51–62. https://doi.org/10.3354/cr01220.
Lin, Z.L., Xu, H.Q., 2017. A study of urban Heat Island intensity based on local climate zones. J. Geo. Inform. Sci. 5 (19), 713–722. https://doi.org/10.3724/SP.J.1047.2017.00000.

Lutz, W., 2017. How population growth relates to climate change. Proc. Natl. Acad. Sci. 114 (46), 12103–12105. https://doi.org/10.1073/pnas.1717178114.

Manob, D., Arijit, D., 2020. Assessing the relationship between local climatic zones (LCZs) and land surface temperature (LST) – a case study of Sriniketan-Santiniketan planning area (SSPA), West Bengal, India. Urban Clim. 32, 100591. https://doi.org/10.1016/j.uclim.2020.100591.

Marie-Leen, V., Matthias, D., Hans, H., Christoph, B., Josef, C., Alexandra, S., et al., 2018. The potential of local climate zones maps as a heat stress assessment tool, supported by simulated air temperature data. Landsc. Urban Plan. 178, 183–197. https://doi.org/10.1016/j.landurbplan.2018.06.004.

Miller, A.W.D., Grant, C.E.H., Muths, E., Amburgey, M.S., Adams, J.M., Joseph, B.M., et al., 2018. Quantifying climate sensitivity and climate-driven change in north American amphibian communities. Nat. Commun. 9 (1). https://doi.org/10.1038/s41467-018-06157-6.

MOHURD, 2016. Notice of the Ministry of Housing, Urban and Rural Construction of the national development and reform commission on printing and distributing action plans for urban climate change. http://www.mohurd.gov.cn/wjfb/201602/t20160224_226732.html (Accessed 15 December 2019).

Natasha, P., Alicia, M.C., 2019. Improving urban planning in a middle temperate Argentinian City: combining urban climate mapping with local climate zones. In: Henríquez, C., Romero, H. (Eds.), Urban Climates in Latin America. Springer, Cham.

Oke, T.R., 1982. The energetic basis of the urban heat island. Q. J. Roy. Meteorol. Soc. 108 (455), 1–24. https://doi.org/10.1002/qj.49710845502.

Pacifici, M., Rama, F., Marins, K.R.D.C., 2019. Analysis of temperature variability within outdoor urban spaces at multiple scales. Urban Clim. 27, 90–104. https://doi.org/10.1016/j.uclim.2018.11.003.

Park, Y.C., Lee, K.D., Asawa, T., Murakam, A., Kim, G.H., Lee, K.M., et al., 2019. Influence of urban form on the cooling effect of a small urban river. Landsc. Urban Plan. 183, 26–35. https://doi.org/10.1016/j.landurbplan.2018.10.022.

Perera, N.G.R., Emmanuel, P.R.M., 2018. A"local climate zone"based approach to urban planning in Colombo, Sri Lanka. Urban Clim. 23, 188–203. https://doi.org/10.1016/j.uclim.2016.11.006.

Qiao, Z., Wu, C., Zhao, D.Q., Xu, X.L., Yang, J.L., Feng, L., et al., 2019. Determining the boundary and probability of surface urban Heat Island footprint based on a logistic model. Remote Sens. (Basel) 11 (11), 1368. https://doi.org/10.3390/rs11111368.

Qiao, Z., Liu, L., Qin, Y.W., Xu, X.L., Wang, B.W., Liu, Z.J., 2020. The impact of urban renewal on land surface temperature changes: a case study in the Main City of Guangzhou, China. Remote Sens. (Basel) 12 (5), 794. https://doi.org/10.3390/rs12050794.

Qin, Z.H., Karnieli, A., Berliner, P., 2001. A mono-window algorithm for retrieving land surface temperature from Landsat TM data and its application to the Israel-Egypt border region. Int. J. Remote Sens. 22 (18), 3719–3746. https://doi.org/10.1080/01431160010006971.

Quan, J.L., Zhan, W.F., Chen, Y.H., Wang, M.J., Wang, J.F., 2016. Time series decomposition of remotely sensed land surface temperature and investigation of trends and seasonal variations in surface urban heat islands. J. Geophys. Res. Atmos. 121 (6), 2638–2657. https://doi.org/10.1002/2015JD024354.

RPC, 2014. Notice of the State Council on adjusting the standards for the classification of cities. http://www.gov.cn/zhengce/content/2014-11/20/content_9225.htm/ (Accessed 15 October 2019).

Shi, Y., Lau, K.K., Ren, C., Ng, E., 2018. Evaluating the local climate zone classification in high-density heterogeneous urban environment using mobile measurement. Urban Clim. 25, 167–186. https://doi.org/10.1016/j.uclim.2018.07.001.

Stewart, I.D., Oke, T.R., 2012. Local climate zones for urban temperature studies. Bull. Am. Meteorol. Soc. 93 (12), 1879–1900. https://doi.org/10.1175/BAMS-D-11-00019.1.

Wang, F., Qin, H.Z., Song, C.Y., Tu, L.L., Arnon, K., Zhao, S.H., 2015. An improved mono-window algorithm for land surface temperature retrieval from Landsat 8 thermal infrared sensor data. Remote Sens. (Basel) 7 (4), 4268–4289. https://doi.org/10.3390/rs70404268.

Wang, Y.S., Zhan, Q.M., Ouyang, W.L., 2017. Impact of urban climate landscape patterns on land surface temperature in Wuhan, China. Sustainability 9 (10), 1700. https://doi.org/10.3390/su9101700.

Wang, R., Ren, C., Xu, Y., Lau, K.K., Shi, Y., 2018. Mapping the local climate zones of urban areas by GIS-based and WUDAPT methods: a case study of Hong Kong. Urban Clim. 24, 567–576. https://doi.org/10.1016/j.uclim.2017.10.001.

Wang, Y.S., Zhan, Q.M., Ouyang, W.L., 2019. How to quantify the relationship between spatial distribution of urban waterbodies and land surface temperature? Sci. Total Environ. 671, 1–9. https://doi.org/10.1016/j.scitotenv.2019.03.377.

World Bank Group, 2015. East Asia's Changing Urban Landscape: Measuring a Decade of Spatial Growth. https://openknowledge.worldbank.org/handle/10986/21159/ (Accessed 26 October 2019).

Wu, Z.F., Dou, P.F., Chen, L.D., 2019a. Comparative and combinative cooling effects of different spatial arrangements of buildings and trees on microclimate. Sustain. Cities Soc. 51, 101711. https://doi.org/10.1016/j.scs.2019.101711.

Wu, X.L., Li, B.X., Li, M., Guo, M.X., Zang, S.Y., Zhang, S.Z., 2019b. Examining the relationship between spatial configurations of urban impervious surfaces and land surface temperature. Chin. Geogr. Sci. 29 (4), 568–578. https://doi.org/10.1007/s11769-019-1055-x.

Yang, X.C., Chen, B.D., Hu, K.J., 2015. Research progress on the impact of urbanization on extreme high temperature events. Prog. Geogr. 34 (10), 1219–1228. https://doi.org/10.18306/dlkxjz.2015.10.002.

Yang, J., Sun, J., Quan, S.G., Li, X.M., 2017. Assessing the impacts of urbanization-associated green space on urban land surface temperature: a case study of Dalian, China. Urban For. Urban Green. 22. https://doi.org/10.1016/j.ufug.2017.01.002.

Yang, J., Wang, Y.C., Xiao, M.X., Jin, C., Xia, J.H.C., Li, X.M., 2019a. Spatial differentiation of urban wind and thermal environment in different grid sizes. Urban Clim. 28 (2019). https://doi.org/10.1016/j.uclim.2019.100458.

Yang, J., Jin, S.H., Xiao, X.M., Jin, C., Xia, J.H.C., Li, X.M., et al., 2019b. Local climate zone ventilation and urban land surface temperatures: Towards a performance-based and wind-sensitive planning proposal in megacities. Sust. Cities Soc. 47 (2019). https://doi.org/10.1016/j.scs.2019.101487.

Yue, W.Z., Liu, Y., Fan, P.L., Ye, X.Y., Wu, C.F., 2012. Assessing spatial pattern of urban thermal environment in Shanghai, China. Stoch. Env. Res. Risk A. 26 (7), 899–911. https://doi.org/10.1007/s00477-012-0638-1.

Yue, W.Z., Liu, Y., Fan, P.L., 2013. Measuring urban sprawl and its drivers in large Chinese cities: the case of Hangzhou. Land Use Policy 31, 358–370. https://doi.org/10.1016/j.landusepol.2012.07.018.

Yvonne, X.Y.N., 2015. A study of urban heat island using" local climate zones"–the case of Singapore. Br. J. Environ. Clim. Change 5 (2), 116–133. https://doi.org/10.9734/BJECC/2015/13051.

Zhan, W.F., Chen, Y.H., Wang, J.F., Zhou, J., Quan, J.L., Liu, W.Y., et al., 2012. Downscaling land surface temperatures with multi-spectral and multi-resolution images. Int. J. Appl. Earth Obs. Geoinf. 18, 23–36. https://doi.org/10.1016/j.jag.2012.01.003.

Zhao, D.X., He, B.J., Christine, J., Mou, B., 2015. Social problems of green buildings: from the humanistic needs to social acceptance. Renew. Sustain. Energy Rev. 51, 1594–1609. https://doi.org/10.1016/j.rser.2015.07.072.